Classification
Physics Abstracts
75.70i — 78.20Ls — 61.16ch

Near-field magneto-optical microscopy

Viatcheslav I. Safarov, Vladimir A. Kosobukin*, Claudine Hermann, Georges Lampel and Jacques Peretti

Laboratoire de Physique de la Matière Condensée, Ecole Polytechnique, 91128 Palaiseau Cedex, France

(Received July 4; accepted November 18, 1994)

Abstract. — A scanning tunneling optical microscope (STOM) operating in total reflexion condition with variable incident angle and polarization sensitive detection of the evanescent mode has been developed to study near-field magneto-optical properties of thin magnetic films. The sample is deposited on the external face of a prism and illuminated in total reflexion conditions with linearly polarized laser light. The evanescent mode close to the surface is detected with a tip-ending monomode optical fiber connected at its other end to a photomultiplier tube equipped with a light-polarization analyzer. The polarization sensitivity of the whole system, which was found to depend on the tip condition, was characterized on the bare prism with s- and p-polarized excitations. The magneto-optical effect in the evanescent mode is measured through a lock-in amplifier by modulating the external magnetic field produced by a coil surrounding the tip. With this set-up we have mainly studied a dielectric garnet film exhibiting perpendicular magnetization. The images, obtained on this sample by measuring the magneto-optical effect under very low amplitude of the external magnetic field modulation, show up submicronic details due to magnetic domain wall motion.

1. Introduction.

The interpretation of near-field images, in particular in terms of surface topography, is generally far from being obvious and sometimes cumbersome. Nevertheless, very recent developments of near-field optical microscopy have led to imaging of magnetic domains with high resolution in thin metallic multi-layer films [1]. It appears that performing the measurement of an externally controlled optical effect, such as Faraday rotation, may be useful for interpreting near-field images.

For that purpose, we have designed a scanning tunneling optical microscope (STOM) operating in total reflexion condition with variable incident angle and with polarization sensitive detection of the evanescent mode [2].

We first discuss the results obtained on a bare prism as a function of excitation polarization and incident angle (beyond the total reflexion limit). These measurements, characteristic of the

* *Permanent address*: A.F. Ioffe Physico-Technical Institute, 194021 Saint Petersburg, Russia.

coupling between a quartz tip scanning the illuminated surface and the evanescent mode, are strongly depending on the tip conditions.

We then show the near-field magneto-optical images of magnetic domains in dielectric garnet films that we have obtained in total reflexion geometry. These images evidence submicronic details related to domain wall motion under magnetic excitation.

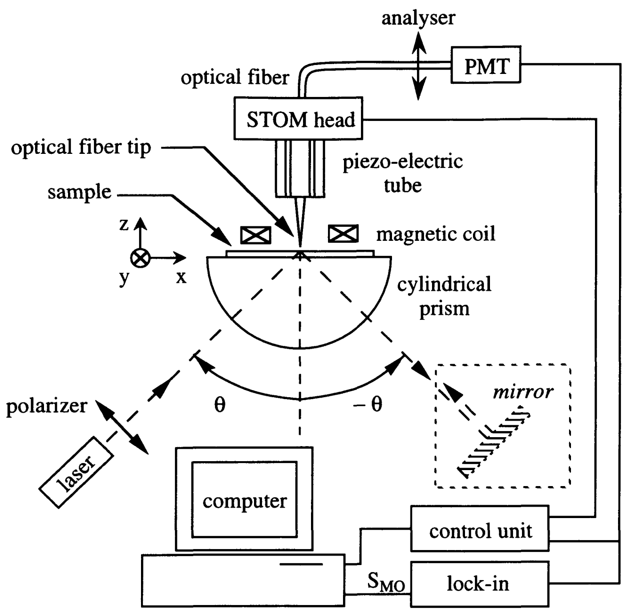

Fig. 1. — Schematics of the scanning tunneling optical microscope set-up.

2. Experimental set-up.

The near-field experiment that we built up basically operates in total reflexion geometry which is the so-called STOM geometry [3]. This set-up is schematized in figure 1. A linearly polarized light illuminates the sample, deposited on the external face of a semi-cylindrical prism, at a variable incident angle θ beyond the total reflexion limit. The evanescent mode close to the sample surface is collected by a tip-ending monomode optical fiber which guides the light to a photomultiplier tube (PMT) equipped with a polarization analyzer. The tip, obtained by chemical etching of the fiber, is mounted on a piezo-electric tube which allows fine x, y, z motions, while larger scale motions of the microscope head are insured by micrometric mechanical displacements. A small coil surrounding the tip produces the external magnetic field perpendicular to the film plane. Under alternative current operation, the magnetic structure of the sample is periodically changed. The resulting light-polarization modulation induced by the magneto-optical effect is transformed into an intensity modulation of the light detected on the PMT through a linear-polarization analyzer, the axis of which makes an angle of 45° with the incident polarization direction. the $d - c$ component of the PMT output signal is used in the feedback loop to maintain a constant average detected intensity. The $a-c$ component of the detector output signal at the frequency of the magnetic field modulation is recorded through a lock-in amplifier and is displayed as the magneto-optical signal S_{MO}. At a point where the magnetization is periodically flipped, this signal can be expressed as follows:

$$S_{\mathrm{MO}} = |E_s|\,|E_p| \cos\left(\Delta\phi_{ps}\right) \tag{1}$$

where E_s and E_p are the amplitude of the two collected components of the evanescent field (one related to the excitation, the other being magneto-optically induced) and $\Delta\phi_{ps}$ is their phase difference.

3. Resolution and polarization sensitivity of the microscope.

3.1 RESOLUTION. — When a mirror is installed perpendicularly to the totally reflected beam, interferences are produced in the evanescent mode close to the surface of the prism. A near-field image of the interference pattern can be obtained by scanning the tip in the x, y plane over the surface and displaying the z-displacement of the tip when the total collected intensity is kept constant (Fig. 2a). This image allows an accurate calibration of the tip motion in the plane of the surface. Moreover by analyzing the amplitude of the intensity modulation along an image line (Fig. 2b), an estimate of the upper limit of the microscope lateral resolution is obtained and found to be better than 66 nm.

3.2 POLARIZATION SENSITIVITY. — The characteristics of the electric field of the evanescent wave at the surface of the bare prism illuminated in total reflexion condition are well known. Indeed, the three components of the field E_x, perpendicular to the incident plane, E_y, in the incident plane and parallel to the surface, and E_z, in the incident plane and perpendicular to the surface, are given by [4]:

$$E_{x,y,z} = T_{x,y,z}\, A_{p,s,p}\, \mathrm{e}^{-z/z_0}\, \mathrm{e}^{-i(\omega t - k_x x + \phi_{x,y,z})} \tag{2}$$

where $A_{p,s,p}$ is the amplitude of the relevant component of the incident field (p-component for E_x and E_z and s-component for E_y). The "transmission" factor $T_{x,y,z}$ and the phase of each component, $\phi_{x,y,z}$, depend on θ and on the prism refractive index, n. The wave vector k_x, which depends on n, λ and θ, evidences that the evanescent wave propagates along the prism surface, in the O_x direction. The evanescent character of this wave appears in the exponential decrease of each field component modulus with the distance, z, to the surface. The decay constant, z_0, which is the same for all the components, also depends on n, λ and θ.

Each component of the evanescent field exhibits a specific variation with θ. Therefore, from the variation with θ of the intensities I_s and I_p measured in near field by the microscope tip, for s- and p-polarization of the incident light, one should be able to identify the components actually collected by the tip and guided by the fiber. As only a relative determination of z (i.e. the displacement of the tip along the direction perpendicular to the surface) can be obtained and as z_0 varies with θ, it is not easy to have an absolute measurement of I_s and I_p in a wide range of the θ values. Therefore, the relevant quantity to be measured is the ratio I_p/I_s which does not depend on z. Two limiting cases can be considered. Either all the components of the field are equivalently collected by the tip or only the components perpendicular to the tip axis, which correspond to transverse waves in the tip, are actually detected. Considering that the amplitudes of the incident light electric field are equal in s- and p-polarization ($A_s = A_p$), the ratio I_p/I_s is given, in the former case, by:

$$\frac{I_p}{I_s} = \frac{T_x^2 + T_z^2}{T_y^2} = R_I\left(2n^2 \sin^2\theta - 1\right) \tag{3}$$

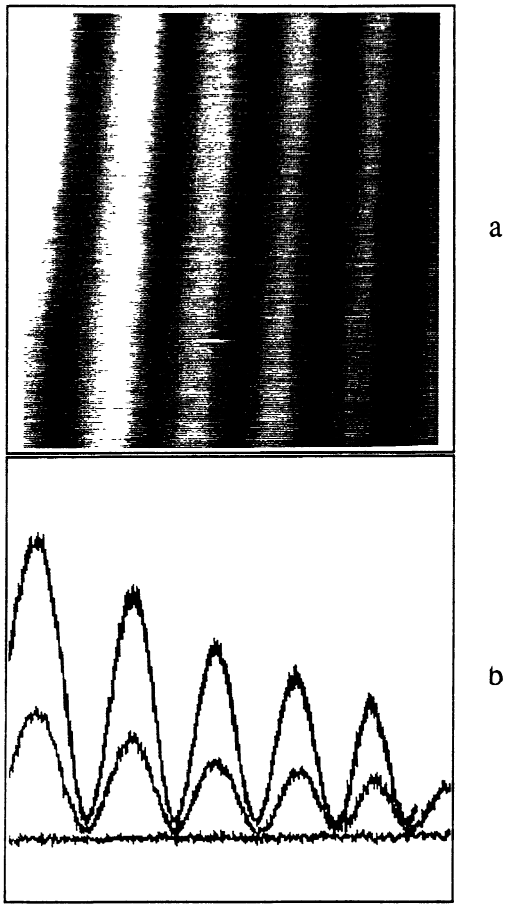

Fig. 2. — a) Interference pattern of two evanescent modes propagating along the prism surface in opposit direction. This near-field image has been obtained by displaying the z-displacement of the tip when the total collected intensity is kept constant. b) One image line: the large modulation amplitude (more than 85%) of the collected intensity indicates that the microscope lateral resolution is better than 66 nm.

whereas, in the latter case, the ratio I_p/I_s is given by:

$$\frac{I_p}{I_s} = \frac{T_x^2}{T_y^2} = R_I\left(n^2 \sin^2\theta - 1\right) \tag{4}$$

where

$$R_I = \frac{n^2 - 1}{\cos^2\theta + n^2\left(n^2 \sin^2\theta - 1\right)} \tag{5}$$

We have measured, with several tips, the ratio I_p/I_s for different values of θ. In figure 3, two typical sets of experimental data are compared with the theoretical variations calculated after equations (3) and (4). It appears that the coupling of the tip with the evanescent field strongly depends on the tip condition. In fact, the tip which collected the whole electric field was a damaged tip while the tip which only collected the components parallel to the surface was a sharp new tip.

One can explain these two behaviors by considering that the only light waves which may be coupled in a sharp tip are transverse waves, i.e. electric field components parallel to the surface, while, in a damaged tip, all the components of the evanescent field may be coupled like in frustrated total reflexion experiments. Of course with other tips we have observed some intermediate behaviors between these two extreme cases.

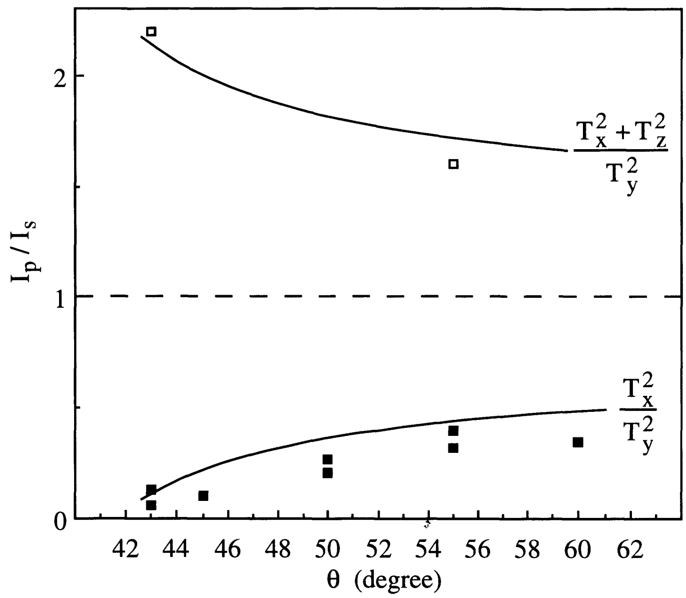

Fig. 3. — Variation of the ratio I_p/I_s as a function of θ. The experimental points have been obtained for two different tips: a sharp new tip (symbols ■) and a damaged tip (symbols □). The full lines represent the theoretical variation calculated after equations (3) and (4).

These results provide a characterization of the tip condition and of the polarization sensitivity of the microscope which are particularly important for performing near-field magneto-optical experiments.

4. Near-field magneto-optics in garnet films.

Garnets, in which magneto-optical effects of large magnitude are currently observed, are transparent to visible light. They can be prepared as thin films ($\approx$ 1 μm), with large size domains (in the μm range) of easy-magnetization axis perpendicular to the film plane, and their magnetic properties are well known [5].

For these reasons we have chosen to study the near-field magneto-optical properties of some of these thin garnet films with 3 μm-wide domains. The sample on the prism surface is illuminated in total reflexion condition with s-polarized light of wavelength λ = 647 nm. Magneto-optical images are obtained by scanning the surface at low frequency with the optical fiber tip, while the magneto-optical effect, in the collected evanescent intensity, is measured as described in paragraph II, for an external magnetic field sinusoidal modulation of small amplitude ($\approx$ 0.3 Oe), at a frequency of 190 Hz.

When the magnetic field is periodically modulated, the relative sizes of the magnetic domains are correlatively modulated which is generally seen as a periodic motion of the domain walls. This induces a periodic variation of the magnetization in the area where the considered wall motion takes place, while elsewhere the magnetization is not modified. Thus, a variation of the magneto-optical effect, at the frequency of the field modulation, occurs only in the region corresponding to the wall motion, which appears as a contrasted region in the image.

This is indeed observed in the magneto-optical image (Fig. 4a). In the grey-level scale of this image, a black point corresponds to a negative lock-in output signal and a white one to a positive signal. The full scale represents a few tenth of a percent of the total collected intensity. The grey parts (zero magneto-optical signal), of about 3 μm width, correspond to the major part of the magnetic domains where the magnetization does not change under low amplitude field modulation, while the white lines (with narrow black borders) image the area where the periodic motion of the domain walls takes place (i.e. where the magnetization changes) under the modulated magnetic excitation. The detail of the magneto-optical signal shape is not yet completely understood but it is possibly related either to the fine magnetic structure of the domain walls or to the characteristics of the evanescent field components and to their coupling with the quartz tip.

The interpretation of the magneto-optical image in terms of visualization of domain wall motion is supported by the following observation. When a large external magnetic field is applied by approaching a permanent ferromagnet, the magnetic domain walls move out of the image which then becomes completely grey (in the whole sample the magnetization is uniform). Then, when the ferromagnet is withdrawn, wall motion features can be again observed in the image (Fig. 4b) but in a configuration (position and shape) generally different from the one existing before the large field was applied. This behavior, which shows that the latter magnetic structure is similarly organized in domains but is not identical to the former one, can be easily observed in standard polarization contrast microscopy.

A remarkable feature of this STOM study is that the near-field magneto-optical images are completely uncorrelated with the near-field topographic image (Fig. 4c) obtained by displaying the z-motion of the tip under feedback conditions (that is maintaining constant the $d-c$ component of the PMT output signal).

5. Conclusion.

The experiments that we have presented show that the measurement of a physical effect, such as Faraday rotation, by modulating the optical properties of the sample, can indeed be useful for interpreting near-field measurements. The same experimental set-up has been used to study magneto-optical effects in a metallic Au/Co/Au sandwich [6]. In this case the interaction of the light electric field with the gold surface plasmon leads to a resonant enhancement of the magneto-optical effects in the evanescent mode, which could lead to image submicronic domains with signal-over-total-intensity ratio as high as a few percent.

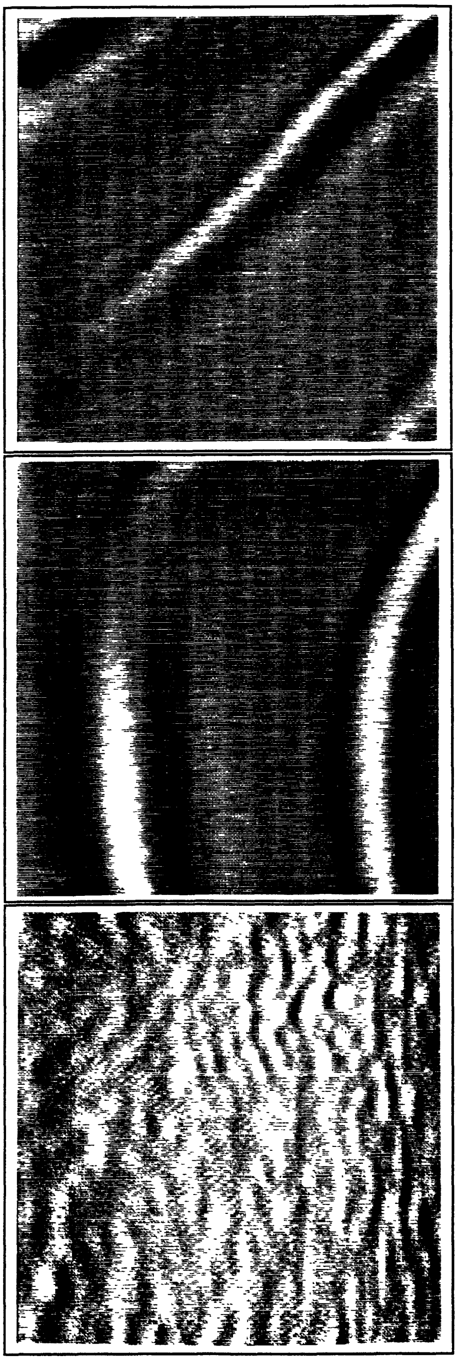

a

b

c

Fig. 4a. — 5 μm $\times$5 μm near-field magneto-optical image of a garnet film measured with an external magnetic field modulation amplitude of 0.2 Oe and with s-polarized incident light. The structures are related to the domain wall motion induced by the magnetic field modulation. b) Magneto-optical image of the same area after applying a large external magnetic field. c) "Topographic" image of the same area obtained by displaying the z-displacement of the tip when the total collected intensity is kept constant.

Acknowledgements.

We are grateful to J. Miltat and A. Thiaville for providing us with garnet samples and for fruitful discussions. We also would like to thank the Direction des Recherches Etudes et Techniques (D.R.E.T.) de la Délégation Générale pour l'Armement (D.G.A.), the Programme Ultimatech, and the Laboratoire Central de Recherche (L.C.R.) of Thomson C.S.F. for financial support. The Laboratoire de Physique de la Matière Condensée is Unité de Recherche Associée D1254 au Centre National de la Recherche Scientifique (C.N.R.S.).

References

[1] Betzig E., Trautman J.K., Wolfe R., Gyorgy E.M., Finn P.L., Kryder M.H. and Chang C.-H., *Appl. Phys. Lett.* **61** (1992) 142.

[2] Preliminary account of the present study has been presented at NFO2 by V.I. Safarov, V.A. Kosobukin, C. Hermann, G. Lampel, C. Marlière and J. Peretti; Proceedings to be published in Ultramicroscopy.

[3] Courjon D., Sarayeddine K. and Spajer M., *Opt. Comm.* **71** (1989) 23;
Reddick R.C., Warmack R.J., Chilcott D.W., Sharp S.L. and Ferrel T.L., *Rev. Sci. Instrum.* **61** (1990) 3669.

[4] Born M. and Wolf E., Electromagnetic theory of propagation and diffraction of light, in Principles of Optics (Pergamon Press, Oxford 1959).

[5] Eschenfelder A.H., Magnetic Bubble technology, in Springer Series in Solid State Sciences, Vol. 14 (Springer Verlag, 1980).

[6] Safarov V.I., Kosobukin V.A., Hermann C., Lampel G., Marlière C. and Peretti J., *Phys. Rev. Lett.* **73** (1994) 3584.